Novel Stoichiometric, Noncovalent Pinacolyl Methylphosphonate Imprinted Polymers: A Rational Design by NMR Spectroscopy

Lucie Malosse,[†] Pascal Palmas,*[,†] Pierrick Buvat,*[,†] Dominique Adès,[‡] and Alain Siove[‡]

CEA, LE RIPAULT, F-37260 Monts, France, and CNRS, Institut Galilée, Université Paris Nord, 99 av. J.B. Clément, 93430 Villetaneuse, France

Received May 26, 2008; Revised Manuscript Received August 18, 2008

ABSTRACT: The stoichiometric noncovalent imprinting of pinacolyl methylphosphonate (PMP), a degradation product of a chemical warfare agent, has been investigated. A rational approach consisting of controlling the number of specific sites produced during the polymerization was carried out in order to design the methacrylic acid (MAA)-based imprinted polymers. The objective of the method was to study by NMR spectroscopy the molecular association process between the monomer (MAA) and the template (PMP) in solution. Accurate variations in the chemical shifts of ^{1}H and ^{13}C were determined in a series of samples at various concentrations in the mixture of acetonitrile/toluene (3:1, v/v). By using an elaborated data treatment, we were able to simultaneously determine the stoichiometry, the association constant, and the condensation degree of the resulting complex. On the basis of these results, a stoichiometric noncovalent PMP-imprinted polymer was subsequently synthesized. Adsorption isotherms of the materials were measured and confronted with those of an imprinted polymer conventionally synthesized with excess monomer. These results established for the first time, the feasibility of imprinted polymers with low-molecular-weight and poorly functionalized templates such as pinacolyl methylphosphonate via stoichiometric noncovalent interactions. Batch binding tests were also carried out on a series of three analogue phosphonates in order to elucidate the influence of the functionality, shape, and size of the analyte on the adsorption properties of the polymers.

Introduction

The molecular imprinting concept has arisen from the ambition to prepare biomimetic materials with selective molecular recognition sites such as those of natural enzymes and antibodies.[1−4] The synthesis of such artificial receptors has thus attracted increasing interest from various research fields, e.g. chromatography,[5−8] solid-phase extraction,[9] catalysis,[10−12] and detection techniques.[1,2,13−16] The preparation of molecularly imprinted polymers (MIPs) involves a first step of complex formation between a template molecule and a functional monomer, followed by polymerization in the presence of a cross-linking agent leading to a three-dimensional network. The extraction of the template and unreacted species renders it possible to obtain the imprinted polymer with substrate-selective cavities that are complementary to the template in terms of size, shape, and functionalities. MIPs obtained by covalent attachment of a template to a monomer generally present well-defined cavities and demonstrated selectivities.[17−19] However, the main limitation of this method is the requirement to synthesize the covalent complex beforehand and then cleave the covalent bonds between both entities without affecting the integrity of the polymeric network. This difficulty can be circumvented if the prearrangement between the template and the monomer is ensured by noncovalent bonds such as ion pairing, hydrogen-bonding, hydrophobic interactions,[20−23] etc. This less restricting method, first introduced by Mosbach in the 1980s permits the imprinting of a very large panel of templates as well as the use of a wide range of monomers. Unfortunately, the apparent simplicity of MIP synthesis by this latter technique has yielded to a generalization of the method and caused people not skilled in the art to comply with a universal recipe. Most often, the rule of thumb dictates a template monomer ratio of 1:4. Alternatively, the trial-and-error method is applied and a series of MIPs with various compositions is prepared so as to select the one with the best properties.[24−26] Because of the weakness of the involved interactions between the template and the monomer, the choice of the experimental conditions (e.g., solvent, concentration, composition, nature of the cross-linker, temperature) becomes a crucial step governing the complex formation process. Rational approaches have already been used for MIP design, e.g. the study of association strengths of the interactions between template and monomer via thermodynamic[27] or UV spectroscopic[28,29] analyses. However, UV spectroscopy cannot be employed when templates do not absorb at appropriate wavelengths, and, in such cases, NMR often represents an interesting alternative. Several research groups have reported on NMR investigations of prepolymerization mixtures for the imprinting of templates such as L-phenylalanine,[30] nicotine,[31] quercetin,[32] 1-benzyluracil,[33] 2,4-dichlorophenoxyacetic acid,[34,35] pteridines,[36] or ampicillin.[37] Most often, these studies have been dedicated to confirming the complex formation, the stoichiometry, and the binding constant, or simply to obtaining a rational understanding of the mechanisms involved in the noncovalent imprinting process. They have generally been performed after the MIP synthesis with the aim of justifying a successful imprint rather than with the objective of selecting the experimental conditions.[32] Furthermore, the calculations are very often carried out by nonlinear curve fittings, thus imposing an a priori assumption of the complex stoichiometry.

The present work reports on an opposite strategy where NMR spectroscopy has been used as a tool to optimize the experimental conditions for the synthesis of a stoichiometric noncovalent MIP. The complexation of the template-monomer in the prepolymerization mixtures was investigated by NMR according to the molar-ratio method. An NMR data treatment methodology, not requiring any assumption of the possible stoichiometry, was then applied. Interestingly, this enabled the simultaneous determination of the stoichiometry, condensation degree, and binding constant.

* Authors for correspondence. (P.B.) Tel +33 247344485; fax +33 247345168; e-mail: pierrick.buvat@cea.fr or (P.P.) tel +33 247344573; fax +33 247345148; e-mail: pascal.palmas@cea.fr.

[†] CEA, LE RIPAULT.

[‡] CNRS, Institut Galilée, Université Paris Nord.

10.1021/ma801171g CCC: $40.75
Published on Web 10/10/2008

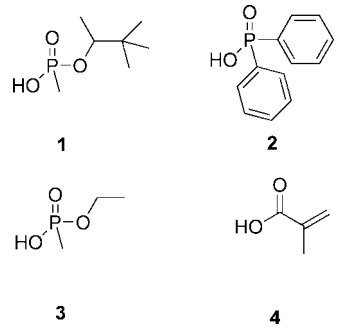

Figure 1. The chemical structures of (1) pinacolyl methylphosphonate (PMP), (2) diphenylphosphinic acid (DPPA), (3) ethyl methylphosphonate (EMP), and (4) methacrylic acid (MAA).

Pinacolyl methylphosphonate (PMP) was used as the target molecule and methacrylic acid (MAA) as the functional monomer (Figure 1). PMP, a low molecular-weight and poorly functionalized molecule, was of interest since it is the hydrolysis product of the neurotoxic chemical warfare agent Soman. The resultant imprinted polymer coupled to an appropriate fluorescent transducer was to be dedicated to the detection of organophosphorus-based chemical warfare agents. Accordingly, it should be emphasized that MIPs developed for chemical sensing applications require various characteristic properties that do not necessarily represent requirements for other applications (e.g., chromatography). More specifically, the sensitive imprinted layer should develop a high affinity for the target analyte with a binding site population that is as homogeneous as possible. The nonspecific interactions should be kept to a minimum[2] since specific recognition needs to occur at the first attempt. Indeed, direct detection precludes the use of selective washing steps as in chromatography or solid-phase extraction.[9] Therefore, particular attention has been paid to the rationalization and optimization of the template-monomer association process in order to reduce the contribution of nonspecific interactions to as large a degree as possible. A previous paper first described the synthesis of PMP-imprinted microspheres by precipitation polymerization with a conventional PMP/MAA ratio of 1:4.[38] In the present study, we investigated the association process between PMP and MAA by hydrogen bonding through analysis of chemical shifts by NMR spectroscopy on a series of PMP and MAA solutions of varying composition. The rationalization of the synthesis conditions were then applied to the preparation of a stoichiometric noncovalent MIP demonstrating an improved selectivity as compared to the MIP synthesized under conventional conditions. The generalization of the methodology presented in this article could be useful as a guide for the rational design of noncovalent imprinted polymers.

Experimental Section

Materials. Pinacolyl methylphosphonate (PMP), ethyl methylphosphonate (EMP), diphenylphosphinic acid (DPPA), 2,2′-azobis(2-methylpropionitrile) (AIBN), 4-methylumbelliferone (4MU), sodium hydroxyde pellets, bromothymol blue, anhydrous toluene, and acetonitrile were purchased from Sigma Aldrich (St. Quentin Fallavier, France) and used without further purification. Hydrochloric acid 1 N, acetone, chloroform, methanol, and absolute ethanol were obtained from VWR (Fontenay-sous-bois, France). Methacrylic acid (MAA) and divinylbenzene (DVB80) from Sigma Aldrich were distilled under vacuum and stored at −20 °C. Anhydrous toluene-d_8 (99.94% D, water content <0.02%), and acetonitrile-d_3 (99.96% D, water content <0.02%) were purchased in 750 μL ampoules from Eurisotop (Saint-Aubin, France).

NMR Titrations. NMR titrations were performed using PMP, freshly distilled MAA, and a mixture of acetonitrile-d_3/toluene-d_8 (3:1, v/v). A preliminary study has shown that the presence of water strongly influences both the complex formation as well as the chemical shifts of the acidic protons. Consequently, samples were prepared in a humidity-controlled glovebox so as to limit the water content as much as possible. For self-titration of MAA, a series of MAA solutions in deuterated solvents (toluene and an acetonitrile/toluene mixture) were prepared in vials by weighing the MAA and solvent so as to obtain a concentration range of 0.03−3 M. For the titration of PMP with MAA, stock solutions of 0.7 M PMP and 3.5 M MAA were prepared and fractioned into a series of 700 μL samples. The final solutions displayed an MAA/PMP molar ratio ranging from 0 to 30 and a constant overall concentration of PMP of 0.1 M. All NMR measurements were carried out at room temperature on a Bruker Avance 200 as well as an Avance 400 WB spectrometer. A standard Bruker switchable QNP probe was employed for 5-mm-diameter tubes. The ^{1}H and ^{13}C chemical shifts were calibrated according to PMP *tert*-butyl protons (^{1}H: 1.133 ppm; ^{13}C: 24.76 ppm) used as a secondary reference. These values were determined with respect to TMS, 0 ppm, and were shown to be independent of the MAA concentration (the difference in chemical shift was determined to be less than 0.01 ppm between two extreme samples with the lowest and highest concentrations of MAA).

PMP-Imprinted Polymers Preparation. The synthesis of the PMP-imprinted microspheres by precipitation polymerization has been described elsewhere[38] and will not be further detailed here. For the synthesis of the PMP-imprinted bulk polymer, template (PMP, 2 mmol, 360 mg), monomer (MAA, 2 mmol, 172 mg), cross-linker (DVB80, 10 mmol, 1.3 g), and initiator (AIBN, 106 mg) were introduced with 2.2 mL of an acetonitrile/toluene mixture (3:1, v/v) in a round-bottomed flask. The components were degassed in an ultrasonic bath for 5min and then purged with argon while being cooled in an ice bath during 10min. The tightly capped flask was then immersed in an oil bath at 60 °C for 18 h. The resultant monolith was crushed and hand ground with a mortar and pestle. The template and the unreacted species were removed by Soxhlet extraction with a mixture of methanol/acetic acid (9:1 v/v). The MIP particles were then rinsed several times with methanol until a neutral pH was reached and finally with acetone before being dried overnight at 50 °C under vacuum. A nonimprinted control polymer (NIP) was synthesized following the same protocol but without the template.

Nitrogen Adsorption Porosimetry. The washed and dried polymers were degassed for 16 h at 50 °C and analyzed by nitrogen adsorption porosimetry (Tristar 3000, Micromeritics). Surface areas were obtained by the Brunauer−Emmett−Teller (BET) method and pore size distributions were determined by the Barrett−Joyner−Halenda (BJH) method.

Functional Group Titrations. The carboxylic acid functions of MAA incorporated into the polymers were titrated by incubating 30 mg of MIP or NIP with 10 mL of a 0.01 M NaOH solution in a mixture of water/acetonitrile (1:1, v/v). The suspensions were agitated on a rocking table overnight at room temperature and then filtered through a 0.45 μm filter. The excess NaOH was titrated with a 1 mM HCl solution in the presence of a few drops of a bromothymol blue solution.

Infrared Spectroscopy. Infrared spectra of the imprinted and nonimprinted polymers were obtained from KBr pellets of the polymers and recorded at room temperature on a Bruker Equinox 55 spectrometer. Infrared spectra of MAA solutions in toluene or in a mixture of deuterated acetonitrile/toluene (3:1, v/v), as well as of the same PMP/MAA mixtures as those used for the NMR titrations, were recorded at room temperature on a Bruker spectrometer. The background was acquired on air after a 10 min purge with nitrogen, and the spectra of the samples were obtained within a 200 μm optical-length liquid cell also after purging with nitrogen for 10 min.

Batch Binding Experiments. The adsorption of PMP (**1**) and EMP (**3**) from toluene solutions was assessed by batch binding tests. Fifteen milligrams of MIP was suspended in 1 mL of the phosphonate solution in toluene at concentrations ranging from 0.5 to 3 mmol/L. A series of NIP samples was also prepared under identical conditions. All the samples were agitated on a rocking

table overnight at room temperature, after which they were filtered through a 0.45 μm filter. The concentration of phosphonate that remained in solution was measured by a previously described technique based on fluorescence.[38] Similar batch binding tests were conducted in chloroform with DPPA because of its insolubility in toluene. Free DPPA was evaluated by UV−visible absorbance measurements at 266 nm. The quantity of phosphonate fixed by the polymer particles was simply calculated as $Q(\mu\text{mol/g}) = (C_i - C_{res})V/m_p$, where C_i, C_{res}, V, and m_p, represents the initial analyte concentration (μmol/mL), the residual analyte concentration after incubation (μmol/ml), the volume of solution (mL), and the mass of polymer (g), respectively.

Results and Discussion

Determination of the Complex Stability by NMR. Measurements of the molecular complex stability and binding constants by various methods have been reviewed by Connors.[39] When a substrate S is partitioned between two states in solution (e.g., a free state S and a complexed state SL in the case of a 1:1 complex formation equilibrium), each nucleus undergoes a chemical exchange between the two states. If the exchange rate is sufficiently low, the NMR spectrum contains two separated lines at two chemical shifts δ_S and δ_{SL}, of which the integration provides a direct measure of the complex concentration. Conversely, if the exchange is fast (i.e., if the rate, expressed in hertz, is higher than the frequency difference between the two NMR resonances of the S and SL species), a single response is observed with a chemical shift δ_{obs} located at the average of δ_S and δ_{SL}, weighted by the molar fractions f_S and f_{SL} of both species: $\delta_{obs} = f_S\delta_S + f_{SL}\delta_{SL}$. Nevertheless, by measuring the NMR chemical shifts on a series of solutions at various monomer concentrations, it is possible to determine the concentration, stoichiometry, and association constant of the complex. The continuous variations method (Job's plot analysis) and the mole ratio method are the two main techniques applied for this purpose. Job's method consists of preparing equimolar solutions of template and monomer at various molar ratios and calculating the complex concentration by using the chemical shifts from NMR analysis.[23,31,34,35,40,41] The complex concentration is then plotted against the template molar fraction, and the extremum gives the stoichiometry. The mole ratio method consists of first preparing a series of mixtures for which the template concentration is held constant and the monomer concentration is increased.[30,33,36,37,41−43] The chemical shift is subsequently plotted as a function of the monomer/template ratio and examined for significant changes corresponding to the stoichiometric ratio. The mole ratio method has the advantage over Job's method in that it permits an evaluation of the association constant once the stoichiometry of the complex has been determined. This latter method was thus chosen and applied to the study of interaction between PMP and MAA. It is noteworthy that for both methods, the approach is not limited to the chemical shifts but can also be extended to other suitable properties such as scalar J couplings, relaxation rates (the inverse of longitudinal relaxation time T_1 or transversal T_2 and the relaxation times in the rotating frame), or self-diffusion coefficients. Nevertheless, the examination and comparison of these possibilities is beyond the scope of the present paper and will be presented elsewhere.

Dimerization of Methacrylic Acid. Methacrylic acid, a very common functional monomer used in MIP preparation, is known for its tendency to form dimers. This feature was of primary importance for the template monomer prearrangement step, and preliminary NMR measurements were thus carried out on a series of MAA solutions to evaluate the MAA self-association equilibrium.

Assuming equilibrium between the monomer (L) and a dimer (L_2):

$$2L \rightleftharpoons L_2$$

the dimerization constant K_{dim} is defined as

$$K_{dim} = \frac{[L_2]}{[L]^2} \quad (1)$$

where [L] and [L_2] are the free MAA and dimer equilibrium concentrations, respectively.

The conservation of total ligand concentration L_t (which corresponds to the known value of MAA introduced) gives:

$$L_t = [L] + 2[L_2] \quad (2)$$

eq 2 can be rewritten as:

$$L_t = [L] + 2K_{dim}[L]^2 \quad (3)$$

For a given value of K_{dim}, this equation has the solution

$$[L] = \frac{1}{4K_{dim}}(\sqrt{1 + 8K_{dim}L_t} - 1) \quad (4)$$

In the fast-exchange limit, the observed NMR chemical shift of a given nucleus is expressed by the simple relation:

$$\delta_{obs} = f_L\delta_L + f_{L_2}\delta_{L_2} \quad (5)$$

where f_L and f_{L_2} are the molar fractions, and δ_L and δ_{L_2} the chemical shifts of the monomer and the dimer respectively. The combination of the fraction $f_{L_2} = 2[L_2]/L_t$ with eqs 1 and 5 leads to:

$$\delta_{obs} = \frac{2K_{dim}[L]^2}{L_t}(\delta_{L_2} - \delta_L) + \delta_L \quad (6)$$

A determination of K_{dim} from experimental data can be made by fitting the observed chemical shift δ_{obs} vs [L] with the analytical expressions 4 and 6 (for this purpose, the nonlinear regression of Origin 7 SR2 (Originlab Corporation, Northampton, MA) was used). A second method consists of plotting δ_{obs} against $f_{L_2} = 2K_{dim}[L]^2/L_t$, where the free monomer concentration [L] is calculated with eq 4 for a given value of K_{dim}. According to eq 6, the best straight line is then obtained for the correct value of K_{dim} (Figure 2).

These two possible treatments were applied to the variations of the chemical shift of the acidic proton of MAA both in toluene-d_8 and in a mixture of CD_3CN/toluene-d_8 (3:1 v/v). Respective values for the dimerization constant of 8 M^{-1} and 0.3 M^{-1} were calculated in these solvents. This difference in

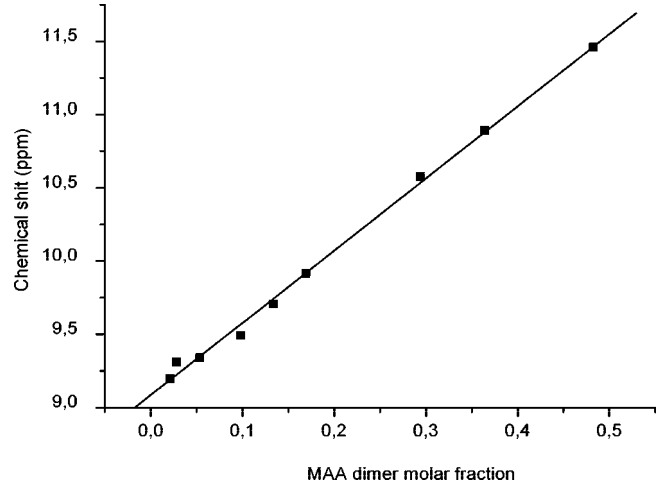

Figure 2. A representation of the acidic proton chemical shift of MAA, measured in a mixture of acetonitrile/toluene, as a function of the dimer molar fraction $f_{L_2} = 2K_{dim}[L]^2/L_t$ with $K_{dim} = 0.3$ M^{-1}.

K_{dim} was consistent with the more polar nature of acetonitrile as compared to toluene which stabilized hydrogen bonds. Ansell has previously reported on the dimerization of MAA in deuterated chloroform[43] and found that the variations in ^{13}C chemical shifts for carboxylic acid fit an association constant of 1200 M^{-1}. Such a discrepancy between the values could be explained by the dissimilarity in solvent polarity. Indeed, the dimerization of other compounds, such as α-caprolactam or acetanilide, was previously studied by NMR spectroscopy in various solvents (chloroform, acetone, acetonitrile), and it was observed that the dimerization constants decrease in going from chloroform to acetonitrile, i.e. in the order of increasing solvent dielectric constant.[44,45] It was also suggested that in the system of α-caprolactam in chloroform, the solute−solute dimerization probably coexists with solute−solvent complexation. This may also be the case with MAA and chloroform, the latter being a good proton-donor.

The results from the present study were also confirmed by infrared spectroscopy measurements performed on the same samples. The examination of the carbonyl group absorption (stretching mode) showed a single band at 1697 cm^{-1} in toluene, while two separate components were clearly visible in the acetonitrile/toluene mixture (3:1, v/v). The first, which was also the most intense, was situated at 1725 cm^{-1}, and a shoulder was observed at 1697 cm^{-1}. This shoulder grew into a well-resolved band at increasing MAA concentrations. The shift to lower frequency of the stretching vibration band in toluene was characteristic of a hydrogen-bonded dimer formation (the band at 1697 cm^{-1} corresponding to the C═O stretching of a cyclic dimer and the band at 1725 cm^{-1} to the C═O stretching of a free COOH).

To conclude, both NMR and IR measurements demonstrated that the dimerization of the MAA molecules was reduced in the mixture of acetonitrile and toluene, rendering the monomer more available for interaction with the template molecule. This solvent mixture was thus chosen for studying the interaction between PMP and MAA. It was all the more interesting that this particular solvent system is known for giving rise to highly porous MIPs.[38] Furthermore, considering the low level of the dimerization constant, the self-association of MAA was, as a first approximation, neglected in the subsequent study.

Investigation of the Interactions between MAA and PMP. Both MAA and PMP offer two possible sites for hydrogen bond interaction. Accordingly, 1:1, 1:2 or 2:1 PMP/MAA complexes can be envisaged a priori as the most plausible forms at the equilibrium, depending on the concentration and the solvent. The molar-ratio methodology based on NMR titration experiments has been carried out to access the actual stoichiometry of the complex and the strength of the association in the acetonitrile/toluene mixture.

As expected, the acidic proton displayed the highest chemical shift variations upon increasing the concentration of MAA. However, since this atom was exchanged between both MAA and PMP, its behavior was not without variation, and its chemical shift first underwent an upfield shift followed by a downfield shift with increasing MAA concentration. The interpretation would require the exchange phenomenon being taken into account in the theoretical formalism. Other ^{1}H nuclei as well as ^{31}P and ^{13}C of PMP underwent smaller changes corresponding to downfield shifts characteristic of hydrogen bonded systems (Figure 3). The variations of the chemical shifts of the protons were roughly proportional to the proximity of the nuclei from the interaction site, in this case the phosphonic acid group. Hence, the methyl protons that were bonded to the phosphorus exhibited strong variations ($\delta_0 \sim 1.637$ ppm), whereas the chemical shift of the more distant *tert*-butyl protons of PMP was almost constant at 1.13 ppm. Conversely, the ^{13}C

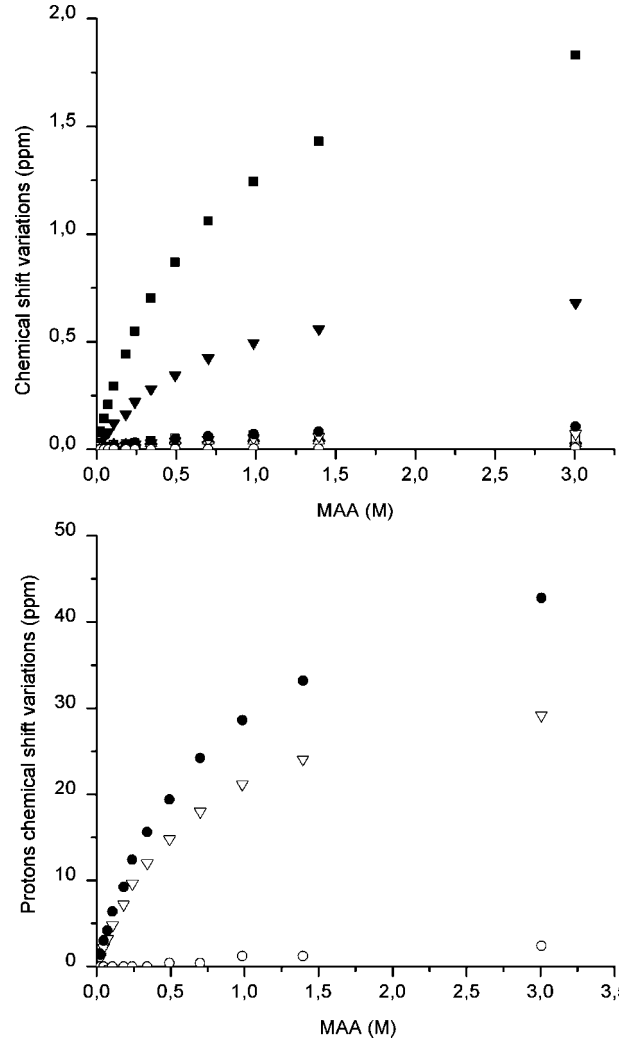

Figure 3. Chemical shifts variations of the various ^{1}H, ^{13}C, and ^{31}P nuclei of PMP upon increasing concentrations of MAA: (■) phosphorus ($\delta_0 \sim 34.189$ ppm); (▼) carbon CHO ($\delta_0 \sim 80.36$ ppm); (●) proton CH_3P ($\delta_0 \sim 1.637$ ppm); (▽) proton CHO ($\delta_0 \sim 4.412$ ppm); (□) carbon C−P ($\delta_0 \sim 11.344$ ppm); (Δ) carbon CH_3-(CHO) ($\delta_0 \sim 16.21$ ppm); (◆) quaternary carbon ($\delta_0 \sim 34.42$ ppm); (○) proton CH_3-(CHO) ($\delta_0 \sim 1.485$ ppm). The notation δ_0 corresponds to the chemical shifts of the nuclei in the PMP solution without MAA.

behavior seemed more complicated since the phosphorus-bonded methyl ^{13}C underwent smaller amplitude variations ($\delta_0 \sim 11.344$ ppm) than the tertiary ^{13}C of PMP (separated from the phosphorus by an oxygen atom, $\delta_0 \sim 80.36$ ppm). This could be due to the lone oxygen pair participating in the hydrogen bond interaction to a certain extent or to the stabilization of the complex formation. However, a molecular modeling calculation of the system would be necessary to verify such eventualities. It is noteworthy that a very small decrease of the J_{C-P} coupling constant (<2 Hz) was observed with increasing MAA concentrations, exhibiting a similar curve shape (not presented in this paper). Measuring the evolution of this parameter, although it may be small, has the advantage of being independent of chemical shift referencing. In fact, this calibration is often a difficult task and has been found to be crucial for accurately measuring small chemical shift differences on a series of samples with a wide range of concentrations.

As described above in the case of the MAA self-association study, an association constant can be derived from the exploitation of the titrations curves presented in Figure 3 by using a numerical fitting procedure. However, this approach often requires a presupposition of the complex stoichiometry. Ramirez

and co-workers have reported on the simultaneous determination of the stoichiometry, the degree of condensation, and the stability constant of relatively weak complexes of molybdenum(VI) by an original data treatment of UV−visible absorbance measurements.[46] Their unique assumption consisted of considering the predominance of a single form of the complex in solution. We adapted this methodology to NMR investigations in order to exploit the titration curves plotted from NMR chemical shift variations. To the best of our knowledge, there exist no reports on the use of such an approach for molecular imprinting studies.

The complex formation can be described by the equilibrium $mS + nL \rightleftharpoons S_mL_n$, with an association constant K:

$$K = \frac{[S_mL_n]}{[S]^m[L]^n} \tag{7}$$

where S and L represent PMP (the substrate) and MAA (the ligand), respectively.

As the concentration of S = PMP was kept constant at S_t and the concentration of L = MAA was increased from zero to a large excess, the maximum of the equilibrium complex concentration was

$$[S_mL_n]_{max} = S_t/m \tag{8}$$

Consequently, the equilibrium complex concentration can be defined as a fraction of this maximum value for any value of the total added MAA concentration $L(x)$:

$$[S_mL_n] = xS_t/m \tag{9}$$

with $0 \leq x \leq 1$.

Equation 7 can thus be rewritten as:

$$f_{m,n}(x) = \frac{L(x) - nS_tx/m}{\left[\frac{x}{m(1-x)^m}\right]^{1/n}} = \left(\frac{1}{KS_t^{m-1}}\right)^{1/n} \tag{10}$$

Practically, for each value of $L(x)$, x can be calculated from the observed chemical shift variation Δ.

Since the hypothesis of a single complex has been made, the observed chemical shift should be:

$$\delta_{obs} = f_S\delta_S + f_{S_mL_n}\delta_{S_mL_n} \tag{11}$$

where δ_S and $\delta_{S_mL_n}$ are the chemical shift in the free PMP state and in the complex state, respectively and f_S and $f_{S_mL_n}$ are their respective molar fractions. Equation 11 can be expressed as:

$$\Delta = f_{S_mL_n}\Delta_{max} \tag{12}$$

where $\Delta = \delta_{obs} - \delta_S$ and $\Delta_{max} = \delta_{S_mL_n} - \delta_S$.

The identity $f_{S_mL_n} = x$ is readily demonstrated, and thus x can be calculated with eq 12.

The technique consists of plotting the funtion $f_{m,n}(x)$ for various (m,n) pairs: only the correct values of m,n will satisfy eq 10, i.e. $f_{m,n}(x)$ is a constant. As can be seen from Figure 4, which represents the evaluation of the function $f_{m,n}$ for the combinations $(m,n) = (1,1)$, $(1,2)$, $(2,1)$, and $(2,2)$ calculated with the chemical shift of the CH_3−P protons, constancy is attained only for $m = n = 1$. These results obviously establish that a 1:1 PMP/MAA complex was formed with an association constant calculated to $K = 1.4 \pm 0.2\ M^{-1}$. Equation 10 provides various possibilities to further ascertain this conclusion. First of all, the curves corresponding to the functions f_{α_m,α_n} should intersect the $f_{m,n}$ straight-line at $x = m\alpha^{1/(1-\alpha)}$, i.e. at $x = 1/2$ for $\alpha = 2$. As demonstrated in Figure 4, the curve of $f_{2,2}$ effectively intersects $f_{1,1}$ at x=1/2. Other verifications can also be made, such as the evaluation of the limiting values $f_{m,n}(0)$ and $f_{m,n}(1)$ of the various functions $f_{m,n}(x)$. In particular, in the case of a 1:1 stoichiometry, the limiting values of the functions $f_{1,2}$ and $f_{2,1}$ should be $f_{1,2}(0) = 0$; $f_{1,2}(1) = +\infty$; $f_{2,1}(0) = 2/K + S_t$ and $f_{2,1}(1) = 0$, again in agreement with the experimental data of Figure 4.

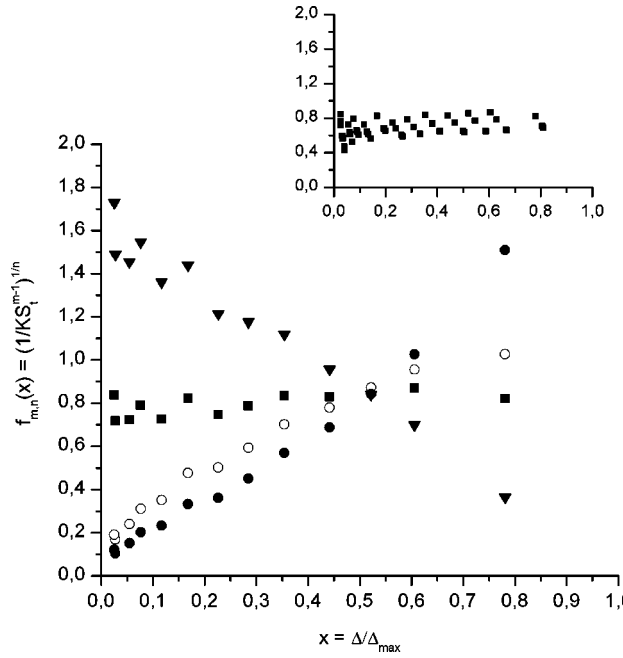

Figure 4. Calculations of $f_{m,n}(x)$ from the chemical shifts of CH_3−P protons for (m,n) values of ■ (1,1), ○ (2,2), ● (1,2), ▼ (2,1). Inset: a superposition of the functions $f_{1,1}(x)$ calculated from the chemical shifts of CH_3−P protons, CH−O proton, CH−O carbon, and phosphorus nuclei.

The calculation of the $f_{m,n}(x)$ functions was applied for the various nuclei of PMP which exhibited significant variations in their chemical shift upon increasing the MAA concentration. Regardless of which nucleus that was considered, the method led to the same stoichiometry and association constant (Figure 4, inset). Usually, single hydrogen bonds show low association constants ($\approx 1\ M^{-1}$), whereas multiple hydrogen bonds induce a stabilization of the edifice and give rise to larger association constants.[23] The 1:1 stoichiometry was thus consistent with the rather low association constant of $1.4\ M^{-1}$, but no conclusions could be drawn as to whether hydrogen bonding occurred via a single bond or via a cyclic hydrogen-bonded system. Moreover, the association constant of PMP and MAA was greater than the MAA dimerization constant ($K = 0.3\ M^{-1}$) and was probably an underestimation of the effective value since the available monomer concentration was actually lower. This confirms that the dimerization of MAA could, as a first approximation, be neglected. Also, the interaction of the cross-linking monomer with the template was required to be negligible in order to preclude nonspecific binding.[28] Divinylbenzene was thus chosen as the cross-linker for the synthesis, as it could not develop specific interactions with PMP. Accordingly, it was not included in the solvent mixture used for the NMR study of the complex stability.

In conclusion, the performed NMR approach successfully permitted the investigation of UV−visible silent molecules. This methodology was particularly useful in the preparation of noncovalent MIPs since it could be readily generalized for other weak complexes. It stands out as a powerful and rapid method for the simultaneous determination of the stoichiometry, the condensation degree, and the association strength, as opposed to Job's plot analysis or nonlinear curve fitting.

Application to the Synthesis of PMP-Imprinted Polymers. Andersson and Nicholls have described the use of UV spectroscopy for analyzing the self-assembly of methacrylic acid and three templates used in the preparation of MIP.[28] Their study

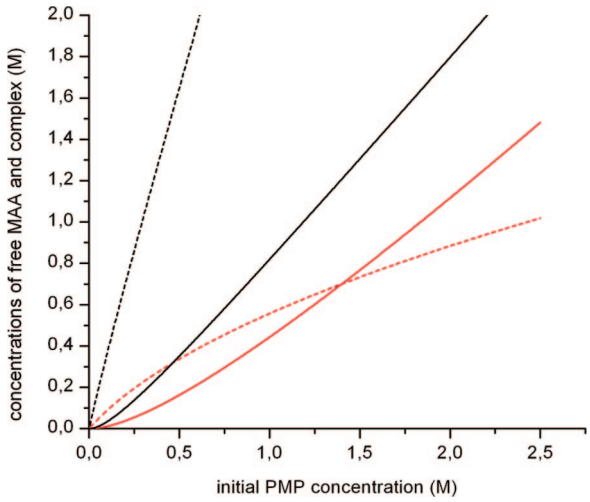

Figure 5. Calculated solution concentrations of free MAA (dashed lines) and PMP/MAA complex (solid lines) for synthesis ratios of PMP/MAA of 1:1 (red lines) and 1:4 (black lines).

demonstrated that the concentration of the complex in the prepolymerization mixture correlated well with the number of specific recognition cavities obtained in the polymer. Accordingly, the difference in relative concentrations of complex and free monomer should be maximized, so as to keep to a minimum the number of nonspecific sites due to randomly incorporated free functional monomer units. Since the 1:1 stoichiometry of the PMP/MAA precursor complex C has been established, the concentrations of free and complexed species should be able to be numerically calculated for various initial conditions. Indeed, the resolution of the equation set:

$$\begin{cases} [\mathrm{MAA}]_0 = [\mathrm{MAA}] + [\mathrm{C}] \\ [\mathrm{PMP}]_0 = [\mathrm{PMP}] + [\mathrm{C}] \\ K = [\mathrm{C}]/[\mathrm{PMP}][\mathrm{MAA}] \end{cases}$$

leads to eq 13 that expresses the concentration of the PMP/MAA complex:

$$[\mathrm{C}] = \frac{1}{2}\left([\mathrm{PMP}]_0 + [\mathrm{MAA}]_0 + \frac{1}{K}\right) - \sqrt{\frac{1}{4}\left([\mathrm{PMP}]_0 + [\mathrm{MAA}]_0 + \frac{1}{K}\right)^2 - [\mathrm{PMP}]_0[\mathrm{MAA}]_0} \quad (13)$$

Equation 13 shows that the amount of complex formed during the prepolymerization step depends on the association constant K, the synthesis template/monomer molar ratio and the initial template concentration. Figure 5 represents the complex and free MAA concentrations calculated against the initial PMP concentration for PMP/MAA ratios of 1:1 and 1:4.

It can be seen from Figure 5 that for a synthesis PMP/MAA ratio of 1:4, the ratio of free MAA to complex increased with the initial PMP concentration. Indeed, the ratio of free MAA to complex could be calculated in retrospect for the MIP prepared by precipitation polymerization with the classical template/monomer ratio of 1:4.[38] This demonstrates that the free MAA concentration was in 74-fold excess over the complex concentration. Such a considerable excess of uncomplexed MAA was assumed to lead to high nonspecific interactions with the analyte, and it was also expected that the fraction of free MAA could be decreased by altering the synthesis conditions. Though the association constant K was rather low, it was thought that instead of using a large excess of monomer to promote the number of specific sites, the initial template concentation could be increased in order to reach a stoichiometric PMP/MAA ratio. With a ratio of 1:1, for initial PMP concentrations greater than 1.5 M, the complex concentration was greater than that of free MAA (Figure 5). Nevertheless, the initial PMP concentration had an upper limit caused by the necessity of a porogen solvent. Indeed, to fulfill the conditions of a PMP/MAA/DVB molar ratio of 1:1:5 and a minimum solvent/monomers ratio of 1:1 v/v, it was calculated that the initial PMP concentration should not exceed 0.56 M. Hence, with a total PMP concentration of 0.5 M and a stoichiometric PMP/MAA ratio, the free MAA concentration was only 2-fold higher than the complex concentration. As quoted above, attention should to be drawn to the fact that chemical sensing applications are directed to the minimization of nonspecific interactions. Accordingly, as the purpose of this study was the development of selective materials for sensing applications, our aim was not to reach a 100% template complexation to increase the number of binding sites but rather to minimize the amount of free functional monomer that was randomly incorporated into the matrix and thus the source of subsequent nonspecific interactions. The fraction of uncomplexed template should not induce nonspecific interactions and was washed out during the extraction process. Hence, the synthesis conditions were chosen as those described by the speciation diagram.

Table 1. A Summary of Certain Characteristics of the Imprinted and Nonimprinted Polymers

polymer	synthesis $[\mathrm{PMP}]_0$ (mol/L)	synthesis PMP/MAA ratio	specific surface area (m^2/g)	COOH capacity (mmol/g)
MIP1	0.01	1:4	650 ± 30	1.4 ± 0.3
NIP 1	0	0:1	680 ± 30	1.2 ± 0.4
MIP2	0.5	1:1	485 ± 25	1.8 ± 0.4
NIP 2	0	0:1	410 ± 20	1.4 ± 0.4

MIP Synthesis and Characterization. A first PMP-imprinted polymer MIP1 (Table 1) was synthesized in previous research efforts by precipitation polymerization, using a conventional 1:4 PMP/MAA ratio and an initial PMP concentration of 0.01 M.[38] This synthesis led to relatively monodisperses microspheres in good yield (65%), with particles diameters ranging from 1 to 10 μm. Following the NMR study described above, a second PMP-imprinted polymer MIP2 was synthesized by using a stoichiometric 1:1 ratio and an initial PMP concentration of 0.5 M (Table 1). This bulk polymerization gave rise to a monolith in 92% yield after workup. Careful structural characterizations were carried out to determine the polymer structure and morphology.

First, nitrogen adsorption porosimetry permitted the determination of the specific surface areas and pore size distributions of the polymers (Table 1). The synthesis processes led to highly porous materials with specific surface areas comprised between 400 and 700 m^2/g. In both syntheses, the surface areas of the MIP and NIP (nonimprinted polymer) were roughly comparable, whereas the bulk synthesis induced lower specific surface areas than the precipitation polymerization. The pore size distributions appeared to be in the microporous range with a population of pores inferior to 2 nm in the four polymers. MIP2 and NIP2 also presented a second population of pores in the mesoporous range, i.e. centered around 50 nm, probably as a result of the grinding process. To fully characterize the chemical structure of the materials, infrared analyses of the four polymers were carried out. The intensity of the infrared spectra was normalized relative to the peak at 710 cm^{-1} corresponding to the C−H bending vibration band of the polystyrene network (Figure 6).

The comparison of the relative intensities of the CH vinyl out of plane bending vibration bands at 988 and 903 cm^{-1} and C═C stretching vibration band at 1629 cm^{-1} from the unreacted vinyl groups revealed that the conversion was higher in the polymers prepared by bulk polymerization. Also, the comparison of the intensities of the C═O stretching vibration bands at 1698 cm^{-1} displayed that the MAA/DVB ratio was roughly equivalent

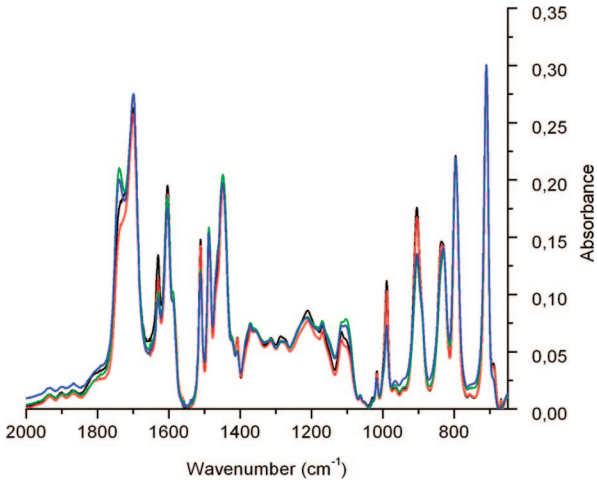

Figure 6. Infrared spectra of MIP 1 (black), NIP 1 (red), MIP 2 (green), and NIP 2 (blue) (KBr pellets) in the 2000−700 cm^{-1} range. The peak assignments were as follows: 1738 cm^{-1} CO stretch, COOH monomeric; 1701 cm^{-1} CO stretch, COOH dimeric; 1630 cm^{-1} vinyl C=C stretch (unreacted vinyl groups); 1603 and 1510 cm^{-1} aromatic C=C stretch; 1487 and 1446 cm^{-1} CH_2 bending; 988 and 903 cm^{-1} CH vinyl out of plane bending; 835, 795, and 710 cm^{-1} aromatic CH bending.

in each polymer. This result has thus demonstrated that the presence of the template molecule did not affect the MAA/DVB copolymerization reactivity ratios, which were both inferior to 1 ($r_1 = 0.124$, $r_2 = 0.602$ with M_1 = styrene and M_2 = MAA[47]) and tended toward an alternating incorporation of the monomers.

In order to ascertain these latter qualitative results, COOH-group titrations were carried out to quantify the number of effective MAA moieties accessible in the polymers. Indeed, it cannot be ruled out that a fraction of the functional units may be trapped in a closed porosity or be made inaccessible by insufficient swelling of the network. During the syntheses, MAA/DVB molar ratios of 1:5 were used. Based on the assumption that the monomers were effectively incorporated in these proportions in the polymers, a theoretical value of 1.36 mmol of COOH groups per gram of polymer was estimated. Considering the experimental error bars, the values listed in Table 1 confirm that the number of acidic groups was roughly the same for all MIPs and NIPs and that it was consistent with both the expected value and the actual results of the infrared spectroscopy. Accordingly, a majority of MAA units seemed to be accessible for rebinding studies. As the interactions between PMP and the imprinted polymers were mainly based on hydrogen bonding via the methacrylic acid moieties, this analysis provided fundamental information concerning the number of accessible functional sites for subsequent rebinding of the analyte as well as a means to later quantify the proportion of effective active sites.

Molecular Recognition. In a first step, the imprinting effect was verified with a batch binding test operated with the template molecule PMP. Figure 7 presents a comparison of the PMP adsorption isotherms for the MIP1, NIP1, MIP2, and NIP2. Both PMP-imprinted polymers displayed a specific rebinding of the molecule as compared to their nonimprinted counterparts. The global capacities of MIP2 and NIP2 were lower than MIP1 and NIP1. Indeed, saturation seemed to have been reached for MIP2 and NIP2 at 40 μmol/g and 20 μmol/g, respectively, whereas the plateau was not yet attained for MIP1 and NIP1. Nevertheless, the difference between MIP and NIP was increased with the rationally designed MIP2 since the amount of PMP bound to NIP2 represented less than 50% of the level of MIP2, to be compared with more than 80% for NIP1 relative to MIP1. As expected, the amount of nonspecific interactions was thus

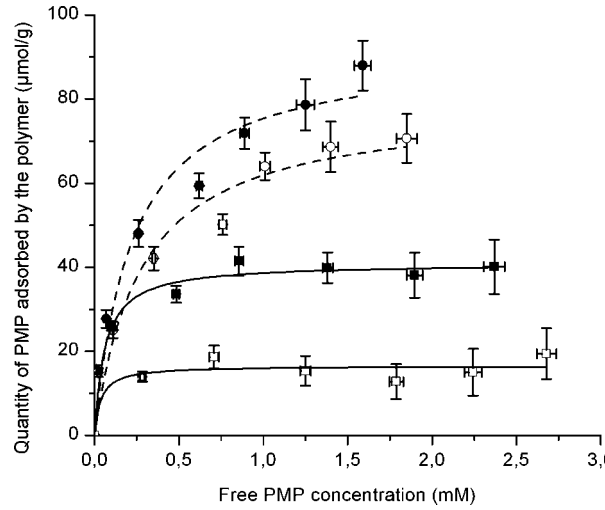

Figure 7. PMP adsorption isotherms (in μmol/g) for (●) MIP 1, (○) NIP 1, (■) MIP 2, and (□) NIP 2.

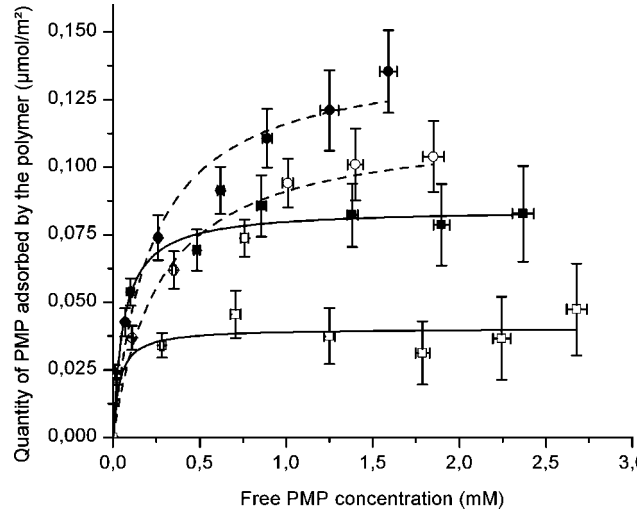

Figure 8. PMP adsorption isotherms (in μmol/m^2) for (●) MIP 1, (○) NIP 1, (■) MIP 2, and (□) NIP 2 after normalization by the specific surface area.

decreased in the optimized MIP2 system, thus proving the efficiency of the approach. Moreover, the adsorption isotherms were normalized by the specific surface areas of the polymers (Figure 8). The imprinting effect remained significant in both systems, demonstrating that the difference in adsorption between MIP and NIP could not be ascribed to their difference in specific surface areas and confirming the existence of specific interactions. Furthermore, the range of the PMP concentration explored in the batch binding test (15 mg of polymer in 1 mL of 0.5−3 mM PMP solutions) corresponded to a solicitation of 0−0.2 mmol/g of COOH units, equivalent to less than 20% of the total amount of COOH units for the four polymers (Table 1). Accordingly, the differences in adsorption could not be ascribed to small variations in the total number of accessible COOH groups. It is noteworthy that the plateau of the adsorption isotherms, e.g. for MIP2, corresponded to approximately 2% of the maximum load capacity.

Eventually, these results proved that a stoichiometric noncovalent imprinting based on weak interactions ($K = 1.4\ M^{-1}$) could still lead to materials with molecular recognition properties. This involves the molecular recognition in imprinted materials not being solely driven by the strength of the interactions between functional groups. Indeed, such an assumption does not take into account the contribution of the

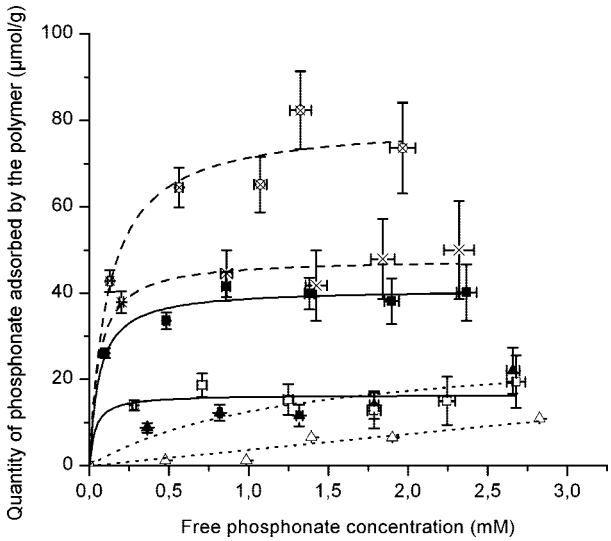

Figure 9. Adsorption isotherms of (■) PMP on MIP2, (□) PMP on NIP2, (▲) DPPA on MIP2, (Δ) DPPA on NIP2, (⊗) EMP on MIP2, and (×) EMP on NIP2.

shape, size, or hydrophobicity of the analyte, nor the Van der Waals interactions. Dickert has already reported on the imprinting of polycyclic aromatic hydrocarbons, exclusively based on Van der Waals interactions.[48] All these parameters should enhance the affinity of the molecule for the polymeric network. To point out the influence of these parameters and to assess the selectivity of the stoichiometric noncovalent PMP-imprinted polymer, batch binding tests with two structural analogues, namely diphenylphosphinic acid (2) (DPPA) and ethyl methylphosphonate (3) (EMP), were carried out (Figure 1). Both substrates possessed a phosphinic acid group susceptible of interacting with MAA moieties, but EMP was smaller than PMP whereas DPPA was bulkier. Figure 9 represents the comparative adsorption isotherms of the three phosphonates for the optimized MIP2 and NIP2.

Ideally, it could be expected from such binding tests that the nonimprinted polymer would not differentiate between the analytes since it is exempt of intrinsic molecular memory. This would result in the level of adsorption by the NIP being identical for the three phosphonates. In return, the MIP is expected to adsorb a greater amount of the phosphonates but to discriminate between the three molecules.

Experimentally, all phosphonates became adsorbed to a lesser degree by the nonimprinted polymer as opposed to by the PMP-imprinted polymer. Consequently, the specific cavities inherent to the imprinting of PMP also enabled the recognition of the same family of compounds by the MIP. Nevertheless, the adsorption level in the NIP differed for the various analytes, proving that the adsorption was not solely dictated by the imprinting process and the functionalities of the polymers and analytes, but also by the morphology and structure. The adsorption of the phosphonates by the polymers was obviously influenced by the size and shape of the molecules. Indeed, DPPA, whose spherical shape was approximately 10 Å in diameter, was discriminated by both MIP2 and NIP2 in comparison with the two other analytes. The phenyl moieties were inflexible as compared to alkyl chains, and therefore the phosphinic acid group that was susceptible of interacting with the MAA units of the polymers was less accessible than in the other molecules. Consequently, the lower level of DPPA adsorption in both MIP2 and NIP2 was probably related to its limited diffusion and its higher hydrophobicity, regardless of the imprinting process. EMP, whose spherical shape was approximately 5−6 Å in diameter, was adsorbed by both MIP2 and NIP2 in greater amounts relative to the imprint molecule PMP, since its smaller size and flexibility enabled it to fit the specific cavities. The imprint, of cylindrical shape, with a diameter of about 5 Å and a height of 10 Å, eventually presented the highest difference between MIP and NIP, i.e. the best imprinting effect.

Conclusions

The present article describes an efficient and novel methodology based on molar-ratio NMR experiments for the quantification of weak complex formations for the preparation of noncovalent imprinted polymers. An efficient data treatment, without a priori, was applied to the titration curves permitting the simultaneous determination of the stoichiometry, the condensation degree, and the stability constant of the self-assembly. This rationalization of template-monomer interactions was applied to the template PMP and the functional monomer MAA, and it was demonstrated that stoichiometric noncovalent imprinted polymers could be obtained with molecular recognition properties, even with weak interactions ($K = 1.4\ M^{-1}$). The described investigations constitute a first step toward a sensitive material for the detection of chemical warfare agent simulants. A next step will consist in the introduction of a fluorescent reporter into the imprinted matrix in order to transduce the presence of the target analyte into the sensitive layer.

Acknowledgment. We thank our co-workers from CEA Le Ripault: V. Frotté from the Laboratoire Expertises Chimiques et Physicochimiques, E. Girard, S. Moulin, and D. Dematteï from the Laboratoire Physico-Chimie for carrying out the nitrogen adsorption experiments, as well as the NMR and infrared spectroscopy analyses.

References and Notes

(1) Dickert, F. L.; Hayden, O. *Trends Anal. Chem.* **1999**, *18* (3), 192–199.
(2) Haupt, K.; Mosbach, K. *Chem. Rev.* **2000**, *100*, 2495–2504.
(3) Sellergren, B. *Molecularly imprinted polymers. Man-made mimics of antibodies and their applications in analytical chemistry*; Elsevier: Amsterdam, 2001.
(4) Yan, M.; Ramström, O. *Molecularly Imprinted Materials. Science and Technology*; Marcel Dekker: New York, 2005.
(5) Sellergren, B. *Trends Anal. Chem.* **1997**, *16*, 310–320.
(6) Sellergren, B.; Shea, K. J. *J. Chromatogr. A* **1993**, *635*, 31–49.
(7) Fischer, L.; Mueller, R. B.E.; Mosbach, K. *J. Am. Chem. Soc.* **1991**, *113*, 9358–9360.
(8) Kempe, M.; Mosbach, K. *J. Chromatogr. A* **1995**, *694*, 3–13.
(9) LeMoullec, S.; Bégos, A.; Pichon, V.; Bellier, B. *J. Chromatogr. A* **2006**, *1108*, 7–13.
(10) Wulff, G. *Chem. Rev.* **2002**, *102*, 1–28.
(11) Slade, C. J.; Vulfson, E. N. *Biotechnol. Bioeng.* **1998**, *57*, 211–215.
(12) Debulis, K.; Klibanov, A. M. *Biotechnol. Bioeng.* **1993**, *41*, 566–571.
(13) Jenkins, A. L.; Uly, O. M.; Murray, G. M. *Anal. Chem.* **1999**, *71*, 373–378.
(14) Li, J.; Kendig, C. E.; Nesterov, E. E. *J. Am. Chem. Soc.* **2007**, *129*, 15911–15918.
(15) Stephenson, C. J.; Shimizu, K. D. *Polym. Int.* **2007**, *56*, 482–488.
(16) Piletsky, S. A.; Piletskaya, E. V.; Panasyuk, T. L.; El'skaya, A. V.; Levi, R.; Karube, I.; Wulff, G. *Macromolecules* **1998**, *31* (7), 2137–2140.
(17) Wulff, G. The covalent and other stoichiometric approaches. In *Molecularly Imprinted Materials. Science and Technology*; Marcel Dekker: New York, 2005.
(18) Wulff, G.; Biffis, A. Molecular imprinting with covalent or stoichiometric non-covalent interactions. In *Molecularly imprinted polymers. Man-made mimics of antibodies and their applications in analytical chemistry*; Elsevier: Amsterdam, 2001.
(19) Whitcombe, M. J.; Rodriguez, M. E.; Villar, P.; Vulfson, E. N. *J. Am. Chem. Soc.* **1995**, *117*, 7105–7111.
(20) Mosbach, K. *Trends Biochem. Sci.* **1994**, *19*, 9.
(21) Sellergren, B. The non-covalent approach to molecular imprinting. In *Molecularly imprinted polymers. Man-made mimics of antibodies and their applications in analytical chemistry*; Elsevier: Amsterdam, 2001.

(22) Yilmaz, E.; Schmidt, R. H.; Mosbach, K. The noncovalent approach. In *Molecularly Imprinted Materials. Science and Technology*; Marcel Dekker: New York, 2005.
(23) Wulff, G.; Knorr, K. *Bioseparation* **2002**, *10*, 257–276.
(24) Takeuchi, T.; Fukuma, D.; Matsui, J. *Anal. Chem.* **1999**, *71*, 285–290.
(25) Lanza, F.; Sellergren, B. *Anal. Chem.* **1999**, *71*, 2092–2096.
(26) Navarro-Villoslada, F.; San Vicente, B.; Moreno-Bondi, M. C. *Anal. Chim. Acta* **2004**, *504*, 149–162.
(27) Whitcombe, M. J.; Martin, L.; Vulfson, E. N. *Chromatographia* **1998**, *47* (7/8), 457–464.
(28) Andersson, H. S.; Nicholls, I. A. *Bioorg. Chem.* **1997**, *25*, 203–211.
(29) Lu, Y.; Li, C.; Zhang, H.; Liu, X. *Anal. Chim. Acta* **2003**, *489*, 33–43.
(30) Sellergren, B.; Lepistö, M.; Mosbach, K. *J. Am. Chem. Soc.* **1988**, *110*, 5853–5860.
(31) Svenson, J.; Karlsson, J. G.; Nicholls, I. A. *J. Chromatogr. A* **2004**, *1024*, 39–44.
(32) O'Mahony, J.; Molinelli, A.; Nolan, K.; Smyth, M. R.; Mizaikoff, B. *Biosens. Bioelectron.* **2006**, *21*, 1383–1392.
(33) Manesiotis, P.; Hall, A. J.; Sellergren, B. *J. Org. Chem.* **2005**, *70*, 2729–2738.
(34) Molinelli, A.; O'Mahony, J.; Nolan, K.; Smyth, M. R.; Jakusch, M.; Mizaikoff, B. *Anal. Chem.* **2005**, *77* (16), 5196–5204.
(35) O'Mahony, J.; Molinelli, A.; Nolan, K.; Smyth, M. R.; Mizaikoff, B. *Biosens. Bioelectron.* **2005**, *20*, 1884–1893.
(36) Quaglia, M.; Chenon, K.; Hall, A. J.; De Lorenzi, E.; Sellergren, B. *J. Am. Chem. Soc.* **2001**, *123*, 2146–2154.
(37) Lübke, C.; Lübke, M.; Whitcombe, M. J.; Vulfson, E. N. *Macromolecules* **2000**, *33*, 5098–5105.
(38) Malosse, L.; Buvat, P.; Adès, D.; Siove, A. *Analyst* **2008**, *132*, 588–595.
(39) Connors, K. A. *Binding constants; The measurement of molecular complex stabilitiy*; John Wiley & Sons: New York, 1987.
(40) Wei, S.; Jakusch, M.; Mizaikoff, B. *Anal. Bioanal. Chem.* **2007**, *389*, 423–431.
(41) Karlsson, J. G.; Karlsson, B.; Andersson, L. I.; Nicholls, I. A. *Analyst* **2004**, *129*, 456–462.
(42) Fu, Q.; Sanbe, H.; Kagawa, C.; Kunimoto, K.-K.; Haginaka, J. *Anal. Chem.* **2003**, *75*, 191–198.
(43) Ansell, R. J.; Kuah, K. L. *Analyst* **2005**, *130*, 179–187.
(44) Chen, J.-S. *J. Chem. Soc., Faraday Trans.* **1994**, *90* (5), 717–720.
(45) Luo, W.-C.; Chen, J.-S. *Z. Phys. Chem.* **2001**, *215* (4), 447–459.
(46) Beltran-Porter, A.; Beltran-Porter, D.; Cervilla, A.; Ramirez, J. A. *Talanta* **1983**, *30*, 124–126.
(47) Brandrup, J.; Immergut, E. H. *Polymer Handbook*, 3rd ed.; John Wiley & Sons: New York, 1989.
(48) Dickert, F. L.; Besenbock, H.; Tortschanoff, M. *Adv. Mater.* **1998**, *10* (2), 149–151.

MA801171G